JOURNAL OF VIROLOGY, Apr. 2005, p. 4033–4042 Vol. 79, No. 7
0022-538X/05/$08.00+0 doi:10.1128/JVI.79.7.4033–4042.2005

Circumventing Tolerance to the Prion Protein (PrP): Vaccination with PrP-Displaying Retrovirus Particles Induces Humoral Immune Responses against the Native Form of Cellular PrP

Daphne Nikles,[1]† Patricia Bach,[2]† Klaus Boller,[2] Christoph A. Merten,[1] Fabio Montrasio,[3] Frank L. Heppner,[4] Adriano Aguzzi,[4] Klaus Cichutek,[1] Ulrich Kalinke,[2]* and Christian J. Buchholz[1]*

Divisions of Medical Biotechnology,[1] Immunology,[2] and Prion Research,[3] Paul-Ehrlich-Institut, Langen, Germany, and Institute of Neuropathology, University Hospital Zürich, Zurich, Switzerland[4]

Received 9 June 2004/Accepted 5 November 2004

Passive immunization with antibodies directed against the cellular form of the prion protein (PrP^C) can protect against prion disease. However, active immunization with recombinant prion protein has so far failed to induce antibodies directed against native PrP^C expressed on the cell surface. To develop an antiprion vaccine, a retroviral display system presenting either the full-length mouse PrP (PrP209) or the C-terminal 111 amino acids (PrP111) fused to the transmembrane domain of the platelet-derived growth factor receptor was established. Western blot analysis and immunogold electron microscopy of the retroviral display particles revealed successful incorporation of the fusion proteins into the particle membrane. Interestingly, retroviral particles displaying PrP111 (PrP^{D111} retroparticles) showed higher incorporation efficiencies than those displaying PrP209. Already 7 days after intravenous injection of PrP^{D111} retroparticles, PrP^C-deficient mice ($Prnp^{o/o}$) showed high immunoglobulin M (IgM) and IgG titers specifically binding the native PrP^C molecule as expressed on the surface of T cells isolated from PrP^C-overexpressing transgenic mice. More importantly, heterozygous $Prnp^{+/o}$ mice and also wild-type mice showed PrP^C-specific IgM and IgG antibodies upon vaccination with PrP^{D111} retroparticles, albeit at considerably lower levels. Bacterially expressed recombinant PrP, in contrast, was unable to evoke IgG antibodies recognizing native PrP^C in wild-type mice. Thus, our data show that PrP or parts thereof can be functionally displayed on retroviral particles and that immunization with PrP retroparticles may serve as a novel promising strategy for vaccination against transmissible spongiform encephalitis.

Prion diseases, also called transmissible spongiform encephalopathies, are a group of fatal neurodegenerative conditions that affect humans and a wide variety of animals. To date there is no therapeutic or prophylactic approach against prion diseases available. However, several recent studies with cell cultures as well as with mice suggest that immunotherapeutic strategies directed against the native cellular form of the prion protein (PrP^C) might be effective in preventing or curing prion diseases (7, 9, 21, 25, 28, 33). Furthermore, recent studies involving transgenic mice with a skewed anti-PrP^C B-cell repertoire (6H4μ) suggest that in principle the immune system does allow the development of PrP^C-specific B cells, even if endogenous PrP^C is expressed (14).

However, active induction of an immune response against native PrP^C or its disease-associated conformer (PrP^{Sc}) has proven to be rather difficult in wild-type mice; i.e., immunization of wild-type mice with recombinant full-length PrP (PrP^{REC}) or peptides thereof resulted in the induction of antibodies that bound PrP^{REC} coated to plastic, but these antibodies failed to recognize native PrP^C as expressed on the cell surface. This phenomenon was further analyzed in different transgenic mouse lines with aberrant PrP expression. Interestingly, among the tested mice, only those expressing PrP under control of an oligodendrocyte and Schwann cell-specific promoter (MBP-PrP mice) were able to mount antibodies directed against native PrP^C (22). In a recall assay, lymph node cells from MBP-PrP mice showed moderate proliferation, whereas lymph node cells from all other PrP-expressing mice tested did not proliferate (22). Since MBP-PrP mice are resistant to prion infection, the protective capacity of actively induced native PrP^C-specific antibodies could not be assessed in that model. Nevertheless, the results suggested that the difficulties in inducing native PrP^C-specific antibody responses most likely resulted from host tolerance to the endogenously expressed PrP^C.

Thus, to overcome host tolerance to PrP^C and to activate PrP-specific B cells, we aimed at defining conditions or immune regimens that resulted in anti-PrP antibody titers in wild-type mice. Reasoning that recombinant virus-like particles (VLPs) are better B-cell immunogens than monovalent recombinant proteins, we developed a retrovirus-based display system for PrP.

C-type retroviruses are enveloped particles that assemble at the plasma membrane. Particle formation is driven by the Gag protein precursor, which is processed by the viral protease to form the matrix protein (MA) and the capsid protein (CA). When expressed in an appropriate eucaryotic environment, the *gag*-encoded proteins self-assemble into noninfectious VLPs which bud from the producer cell in the absence of the viral envelope protein (26). Moreover, retroviruses can incorporate

* Corresponding author. Mailing address for Ulrich Kalinke: Division of Immunology, Paul-Ehrlich-Institut, 63225 Langen, Germany. Phone: 49-6103-772002. Fax: 49-6103-771253. E-mail: kalul@pei.de. Mailing address for Christian J. Buchholz: Division of Medical Biotechnology, Paul-Ehrlich-Institut, 63225 Langen, Germany. Phone: 49-6103-774011. Fax: 49-6103-771255. E-mail: bucch@pei.de.

† D.N. and P.B. contributed equally to this work.

foreign transmembrane proteins into the envelope, as has been shown in the case of human immunodeficiency virus (HIV)-expressing complement regulatory proteins such as CD55 (20). Although the molecular basis for the incorporation of foreign surface molecules in retroviruses is not fully understood, overexpression of surface receptors of Gag-expressing cells is usually one critical requirement.

We used the prototype of C-type retroviruses, murine leukemia virus (MLV), to set up the display of PrP on retrovirus-like particles. We show that upon overexpression of PrP, MLV-derived VLPs that display PrP^C can be generated. Moreover, these PrP retroparticles proved to be highly immunogenic in PrP^C-deficient mice and, even more importantly, evoked native PrP^C-specific antibody responses in wild-type mice.

MATERIALS AND METHODS

Generation of PrP display constructs. For construction of pDisplay (Invitrogen)-based expression constructs, three different coding regions of murine PrP, i.e., amino acids 23 to 231 (PrP209), amino acids 90 to 231 (PrP142), and amino acids 121 to 231 (PrP111), as well as the region encoding amino acids 1 to 52 of the human epidermal growth factor (EGF) molecule, were amplified as 665-, 465-, 376-, and 245-bp PCR fragments, respectively, by using oligonucleotides 5′-GTAT**GGCCCAGCCGGCC**AAAAAGCGGCCAAAGC-3′ (forward 209), 5′-GTAT**GGCCCAGCCGGCC**CAAGGAGGGGGTAC-3′ (forward 142), 5′-GACT**GGCCCAGCCGGCC**GTGGGGGGCCTTGGTGGCTACATGC-3′ (forward 111), 5′-GACTCCGCGGCCTTCCCTCGATGCTGGATCTTCTCCCGTCG-3′ (reverse PrP), 5′-GC**GGCCCAGCCGGCC**GATTATAAGGACGACGATGATAAGGCTAGCGCAATAGTGACTCTGAGTGTCC-3′ (forward EGF), and 5′-TCC**CCGCGG**TGCGGCCGCCCTTCCCTCGATAGC-3′ (reverse EGF) and the PrP-encoding plasmid phgPrP (8) or the EGF-encoding plasmid pTC53-EGF (17) as the template. In these primer sequences, the SfiI and SacII restriction sites are in boldface and the factor Xa cleavage sites are underlined. Upon subcloning of PCR products and sequence verification, SfiI/SacII fragments were ligated into SfiI- and SacII-digested pDisplay (Invitrogen), resulting in the display constructs pD-PrP111, pD-PrP142, pD-PrP209 and pD-EGF.

Cells and mice. Human embryonic kidney (HEK)-293FT cells (Invitrogen, catalog no. R700-07) and murine neuroblastoma N2A cells (ATCC CCL-131) were cultivated in Dulbecco's modified Eagle's medium supplemented with 10% fetal calf serum, benzylpenicillin (60 μg/ml), and streptomycin (100 μg).

PrP-deficient (*Prnp*$^{o/o}$) mice (3) and tg33 transgenic mice overexpressing PrP specifically on T cells (23) were bred under specific-pathogen-free conditions at the central mouse facility of the Paul-Ehrlich-Institut. Unmutated C57BL/6 mice (referred to as wild-type [*Prnp*$^{+/+}$]) were purchased from Charles River Laboratory or were bred at the Paul-Ehrlich-Institut. Heterozygous mice carrying one *Prnp* knockout allele and one wild-type allele (*Prnp*$^{+/o}$) were obtained by crossing *Prnp*$^{o/o}$ mice with C57BL/6 mice. The genotypes of *Prnp*$^{o/o}$ and *Prnp*$^{+/o}$ mice were verified by a combined PCR approach with primers P3 (5′-ATTCGCAGCGCATCGCCTTCTATCGCC-3′), P10 (5′-GTACCCATAATCAGTGGAACAAGCCCAGC-3′), and P3′NC (5′-CCCTCCCCCAGCCTAGACCACGA-3′), identifying the wild-type and the targeted *Prnp* allele as a 500- and 300-bp PCR products, respectively. Experimental mouse work was carried in compliance with the regulations of the German animal protection law.

Production of PrP retroparticles. Three T175 flasks containing HEK-293FT cells grown to subconfluency were transiently cotransfected with the MLV *gag/pol* expression plasmid pHIT60 (29) and the PrP or EGF display construct, respectively. For transfection, 45 μg of each of the two plasmids were mixed with 90 μl of Lipofectamine and 180 μl of Plus reagent (Invitrogen). Cell culture supernatant was harvested twice, at 48 and 72 h after transfection, and particles were concentrated by low-speed centrifugation (3,600 rpm, 4°C, Biofuge; Haereus) or by centrifugation through a sucrose cushion (35,000 rpm, 4°C, Beckman SW41). The pelleted virus was resuspended in 1 ml of phosphate-buffered saline (PBS) and used for electron microscopy, immunization experiments, and Western blot analysis. Sucrose cushion-purified particles and particles concentrated by low-speed centrifugation were equally immunogenic. However, low-speed centrifugation was routinely used, as this resulted in higher particle numbers. For quantification of particle numbers, reverse transcriptase (RT) activity was determined with a C-type RT activity kit (Cavidi Tech), and enzyme-linked immunosorbent assay (ELISA) tests were performed (see below).

Immunofluorescence. N2a cells were transfected and 48 h later were fixed with 2% formaldehyde in PBS. Fixed cells were stained with the anti-PrP mouse monoclonal antibody 6H4 (Prionics) or the anti-human EGF mouse monoclonal antibody EGF-10 (Sigma). To detect the MLV CA protein in double stainings, samples were additionally incubated with the goat anti-MLV p30 serum (Quality Biotech). Fluorescein isothiocyanate (FITC)-conjugated anti-mouse immunoglobulin (Ig) (Dianova) and Cy3-conjugated anti-goat Ig (Dianova) were used as secondary antibodies.

Western blot analysis. Transfected HEK-293FT cells were harvested 48 h after transfection and lysed in radioimmunoprecipitation assay lysis buffer (25 mM Tris [pH 8], 137 mM NaCl, 10% glycerol, 0.1% sodium dodecyl sulfate, 0.5% sodium deoxycholate, 1% NP-40, 2 mM EDTA). The cell culture supernatant was filtered (Sartorius 0.45-μm-pore-size filter), and particles were purified by centrifugation through a sucrose cushion (35,000 rpm, 4°C, Beckman SW41). For deglycosylation, 7.5 μl of concentrated particles was incubated with 10 U of peptide *N*-glycosidase F (PNGase F) enzyme (New England Biolabs). Buffer conditions, incubation times, and temperatures were according to the manufacturer's instructions. Samples were separated on sodium dodecyl sulfate–16% polyacrylamide gels and then transferred to a nitrocellulose membrane (Hybond ECL; Amersham). Protein detection was achieved with the antihemagglutinin (anti-HA) mouse monoclonal antibody 12CA5 (Roche), the anti-PrP monoclonal antibody 6H4 (Prionics), or goat anti-MLV p30 serum (Quality Biotech). As the secondary antibody, horseradish peroxidase (HRP)-conjugated rabbit anti-goat Ig (Dako) or goat anti-mouse Ig (Sigma) was used. Bands were visualized by using the SuperSignalPico chemiluminescence kit (Pierce) and a LumiImager (Roche).

Electron microscopy. For detection of PrP displayed on retrovirus particles, ultrathin frozen sections of virus-producing cells or virions concentrated from the cell supernatant were used. Ultrathin frozen sections were prepared as described by Tokuyasu and Singer (32). Cells were fixed with a mixture of 2% formaldehyde and 0.1% glutaraldehyde for 1 h. After being washed, the fixed cells were embedded in warm liquid agarose, which after gelling could be cut into small blocks. These blocks were immersed overnight in 2.3 M sucrose containing 10% polyvinylpyrrolidone, frozen in liquid nitrogen, and cut into 80- to 100-nm sections with an ultramicrotome (Ultracut E; Reichert, Vienna, Austria) with cryoequipment. Sections were mounted on carbon-coated Formvar grids and, after thawing, washed with PBS. After treatment with 2% bovine serum albumin (BSA), the grids were incubated with the 6H4 antibody at a 1:750 dilution. After being rinsed in PBS, grids were incubated with anti-mouse IgG (1:100 dilution) coupled to 10-nm-diameter gold particles (BioCell). Finally, to embed and stain structures, the grids were floated, sections down, on 1.6% methylcellulose containing 0.2% uranyl acetate for 5 min. Excess methylcellulose was aspirated before the resulting thin film was air dried (10).

For immunonegative staining, 20 μl of virus suspension was adsorbed to glow-discharged carbon-coated Formvar grids for 2 min. After being rinsed in PBS, the grids were incubated with 2% BSA for 30 min and with the 6H4 or anti-EGF primary antibodies at a 1:750 dilution for 1 h. After being washed, grids were incubated with a 1:100 dilution of 10-nm-diameter-gold-labeled anti-mouse IgG (BioCell, Cardiff, United Kingdom) for 30 min. Finally, immunolabeled viruses were negatively stained with 2% uranyl acetate or phosphotungstate for 10 s.

Electron microscopy preparations were examined in a Zeiss EM 109 or 902 electron microscope, and micrographs were taken on Kodak Estar electron microscope film.

Immunization of mice. *Prnp*$^{o/o}$, *Prnp*$^{+/o}$, and C57BL/6 mice, 2 to 3 months of age, were immunized by intravenous (i.v.) injection of approximately 10^{11} retroviral particles displaying PrP111 (PrP^{D111} retroparticles) in 200 μl of PBS. Booster injections were performed 14 days after primary immunization. Blood was taken weekly to monitor the antibody reactivity. For immunizations in the presence of various adjuvants, PrP^{D111} retroparticles were emulsified in an equal volume of cytidylguanyl oligodeoxynucleotides (CpG1668) (50 μg/mouse; 1:2), Titer Max (1:2), alum (1:2), or complete Freund's adjuvant (CFA) and incomplete Freund's adjuvant (IFA) (1:2) immediately before subcutaneous (s.c.) administration (100-μl total volume). All adjuvants were obtained from Sigma. For boosting upon priming with PrP^{D111} retroparticles in CFA, IFA was used.

Analysis of PrP-specific antibodies by ELISA. Expression and purification of recombinant mouse PrP amino acids 121 to 231 ($PrP^{REC121-231}$) was performed as described previously (15, 35). In brief, the expression plasmid pRSETa mPrP(121–231) fused to an N-terminal histidine tag was transformed into *Escherichia coli* BL21(DE3) (Invitrogen). Bacteria were grown to an optical density at 600 nm of 0.5 and then induced with 1 mM isopropyl-β-D-galactopyranoside (IPTG) (Sigma). Cells were harvested 6 h after induction, centrifuged, and resuspended in 6 M guanidinium hydrochloride–5 mM Tris-HCl–100 mM

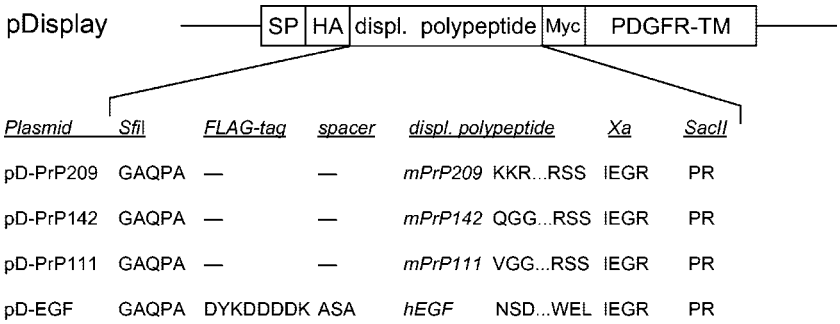

FIG. 1. Schematic representation of the display expression constructs. The pDisplay expression plasmid (Invitrogen) provides the immunoglobulin signal peptide (SP), the HA and Myc tags, and the transmembrane domain of the PDGF receptor (PDGFR-TM). In addition, a factor Xa cleavage site was inserted N terminal to the PDGFR-TM.

Na_2PO_4–10 mM reduced glutathione (pH 8.0). After sonication and centrifugation, the soluble protein fraction was added to a nickel-nitrilotriacetic acid agarose resin (Qiagen) for purification.

The wells of 384-well ELISA plates were coated with 5 μg of $PrP^{REC121-231}$ per ml in PBS and blocked with 5% BSA. Twenty-fold-prediluted sera were serially twofold diluted (20 $\log_2$) in PBS–0.1% Tween–1% BSA and added to the ELISA plates. After 2 h of incubation at room temperature, the plates were thoroughly washed and 1:1,000-diluted HRP-conjugated polyclonal rabbit antibody directed against mouse IgM, IgG, and IgA (anti-mouse IgM+G+A; Zymed) was added. After 1 h of incubation at room temperature plates were washed, and for the detection of bound HRP-coupled antibodies, substrate (0.5 mg of 2,2′-azino-diethylbenzothiazolinsulfonate [Roche] per ml in 0.1 M NaH_2PO_4 [pH 4] and 30% H_2O_2) was added. The optical density was determined at a wavelength of 405 nm.

To quantify molecules displayed on retroparticles, purified PrP or EGF retroparticles were prediluted 1:10 in 0.1 M $NaHCO_3$ (pH 9.6) and then serially threefold diluted (10 $\log_3$) and applied to 96-well ELISA plates (Nunc). Upon blocking with 5% BSA, 6H4 or anti-p30 antibodies prediluted in PBS–0.1% Tween–1% BSA were added and left for 2 h at room temperature. After thorough washing, bound antibody was decorated with 1:1,000-diluted HRP-conjugated rabbit anti-mouse IgM+G+A antibody (Zymed).

Flow cytometric determination of PrP^C-specific serum binding. For flow cytometric determination of PrP^C-specific serum antibody binding, heparinized tg33 mouse blood diluted in PBS–2% fetal calf serum–0.03% NaN_3–20 mM EDTA (pH 8) was incubated for 20 min at 4°C with either sera of immunized mice, 6H4 as a positive control, isotype controls, or normal mouse serum together with phycoerythrin-conjugated anti-CD3 (Caltag). After washing, blood cells were incubated for 20 min at 4°C with FITC-conjugated donkey anti-mouse IgG (Dianova) or goat anti-mouse IgM (Caltag) and then subjected to red blood cell lysis and fixation with fluorescence-activated cell sorter (FACS) lysing solution (Becton Dickinson) according to the manufacturer's instructions. Samples were analyzed on a FACScan machine (Becton Dickinson) by acquiring 10,000 events in the lymphocyte gate. Data analysis was performed with the Cell Quest software (Becton Dickinson).

RESULTS

Generation and characterization of PrP retroparticles. To generate PrP displaying VLPs, expression constructs encoding either the full-length PrP covering codons 23 to 231 (PrP209) or the C-terminal fragment covering codons 90 to 231 (PrP142) or 121 to 231 (PrP111) were generated. For this, fragments encoding the respective PrP portions were ligated into the pDisplay vector, encoding the murine immunoglobulin κ chain signal peptide at the N terminus and the transmembrane domain of the platelet-derived growth factor receptor (PDGFR) at the C terminus (4, 6). Thus, PrP fusion proteins D-PrP111, D-PrP142, and D-PrP209 expressed from the resulting plasmids contained HA and Myc tags for easy detection and a factor Xa cleavage site for preparation of soluble PrP fusion proteins (Fig. 1). We used this strategy initially to produce EGF-displaying retroviral particles, which were used as negative control particles in this study (Fig. 1).

To verify proper expression of the fusion proteins, the human cell line HEK-293FT and the murine neuroblastoma cell line N2a were transiently transfected with plasmid pD-PrP111, pD-PrP209, or pD-EGF and analyzed by immunofluorescence staining. Strong and specific cell surface staining was found for the D-EGF (Fig. 2B) and the D-PrP111 (Fig. 2F) proteins, while only weak signals were detected for the D-PrP209 protein (not shown). Thus, compared to endogenous PrP levels in N2a cells (Fig. 2D), strong overexpression of the D-PrP111 protein was achieved (Fig. 2F). Upon coexpression of the MLV *gag* and *pol* genes, colocalization of the MLV CA protein with the D-PrP111 or the D-EGF molecules at the cell surface was demonstrated (Fig. 2C and G).

To generate retroviral particles displaying the protein D-PrP209, D-PrP142, D-PrP111, or D-EGF, HEK-293FT cells were transfected with the different expression plasmids, pD-PrP209, pD-PrP142, pD-PrP111, and pD-EGF, in combination with pHIT60 (carrying the MLV *gag* and *pol* genes), respectively. As no packagable nucleic acid was provided, noninfectious VLPs were generated. Cell lysates and particle preparations were analyzed by Western blotting using an anti-HA tag-specific antibody and the PrP-specific antibody 6H4. All D-PrP variants showed the typical pattern of at least three different variants of PrP, i.e., un-, mono-, and diglycosylated protein, at the expected molecular weights (Fig. 3A to C). In line with the results of the immunofluorescence analysis, stronger signals were obtained for the D-PrP111 protein, while only faint bands were detected for the D-PrP209 protein (Fig. 3A). In the particle fraction, the D-PrP111 and D-PrP142 proteins as well as the D-EGF protein were readily detectable, suggesting that they were incorporated into retrovirus-like particles. In fact, incorporation of the D-PrP111 protein even seemed to exceed that of the D-EGF protein (Fig. 3B, compare lanes 1 and 2).

Moreover, the incorporated D-PrP111 and D-PrP142 proteins were fully glycosylated (see PNGase F treatment in Fig. 3C, lane 3) and easily detectable by the 6H4 antibody (Fig. 3C, lanes 2, 3, 5, and 6). In contrast, the D-PrP209 protein was incorporated at a considerably lower level. Only when 40-fold-higher particle numbers were used in Western blot analysis did the D-PrP209 protein become detectable (Fig. 3B, lane 3).

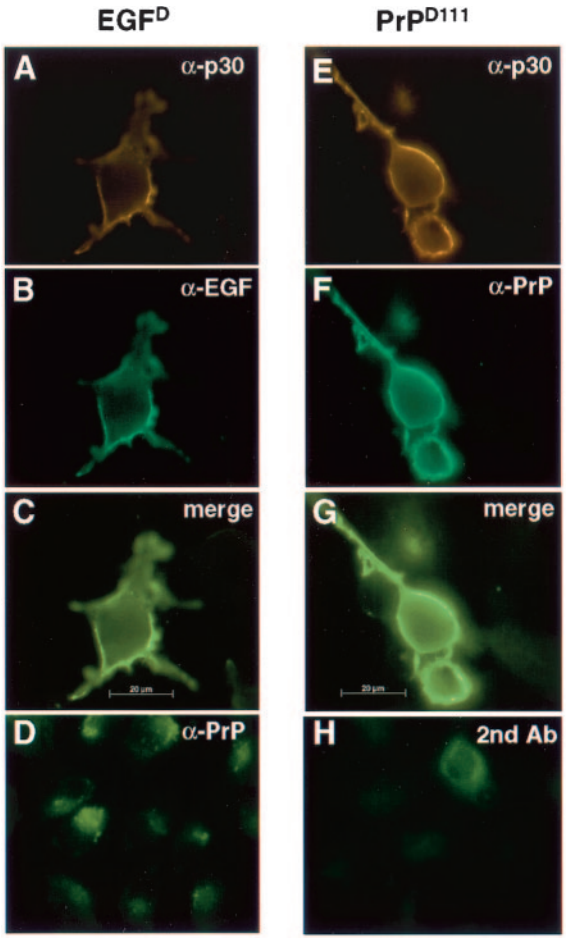

FIG. 2. Display constructs encoding EGF and PrP fusion proteins give rise to high surface expression on transiently transfected N2A cells. N2A cells were transfected with plasmids pD-EGF and pHIT60 (A to D) or pD-PrP111 and pHIT60 (E to H). Cells were stained with anti-PrP (α-PrP) antibody 6H4 (D and F), with anti-EGF antibody (B), or with anti-p30 antiserum (A and E), and bound antibody was detected with FITC-conjugated anti-mouse Ig (B, F, D, and H) or Cy3-conjugated anti-goat Ig (A and E). The merge of A and B is shown in panel C, and that of E and F is shown in panel G.

This was not due to reduced particle release in presence of the D-PrP209 protein, as the MLV capsid protein p30 was found to be present in similar amounts in the cell culture supernatants of pD-PrP209/pHIT60- and pD-PrP111/pHIT60-transfected cells (Fig. 3B). Thus, due to higher cell surface expression levels and increased particle incorporation rates, the D-PrP111 protein allowed the production of particle stocks containing at least 100-fold-larger amounts of PrP than stocks of PrP^{D209} retroparticles.

In addition to Western blot analysis, the particles were subjected to ELISA analysis by applying $\log_3$ dilutions of concentrated stocks (100 RT units/ml) to ELISA plates and analyzing anti-PrP and anti-p30 binding. While PrP^{D111} retroparticles showed strong binding of the PrP-specific 6H4 antibody and of the anti-p30 antibody, EGF^{D} retroparticles showed no 6H4 binding but strong anti-p30 binding (Fig. 3D). Therefore, throughout this study the ELISA was used to standardize particle preparations for immunization purposes.

To further verify the identity of PrP-displaying retroparticles, transfected cells and particle preparations were subjected to electron microscopic analysis using immunogold labeling of the 6H4 antibody. Sections of HEK-293T cells transfected with pD-PrP111/pHIT60 showed a strong and specific accumulation of gold particles along the cell membrane. Gold particles were also found at sites of cytoplasmic extrusions, which in part had a virus particle-like morphology (Fig. 4a). Stocks of PrP^{D111} particles contained particles with a typical C-type retrovirus morphology as well as pleomorphic, vesicle-like structures (Fig. 4b and c). Both were specifically stained at their surrounding membranes. The controls, i.e., PrP retroparticles treated with the gold-labeled antibody only or EGF-displaying particles treated with both antibodies, did not show any staining (data not shown and Fig. 4e), whereas EGF^{D} retroparticles showed specific surface staining with an EGF-specific antibody (Fig. 4d).

Induction of PrP-specific antibody responses in mice. To verify the antigenicity of the PrP^{D111} retroparticles, $Prnp^{o/o}$ mice, which are devoid of endogenously expressed PrP^{C}, and $Prnp^{+/o}$ and $Prnp^{+/+}$ mice, which express either one or two *Prnp* alleles, respectively, were immunized i.v. with approximately 10^{11} PrP^{D111} retroparticles, and serum was taken weekly. Already 7 days after immunization, $Prnp^{o/o}$ mice showed high titers of PrP-specific antibodies as indicated by an ELISA detecting PrP-specific IgM, IgG, and IgA (Fig. 5A). Interestingly, despite the expression of one or two *Prnp* alleles, $Prnp^{+/o}$ and $Prnp^{+/+}$ mice also mounted PrP-specific antibody responses, albeit at substantially reduced levels compared to $Prnp^{o/o}$ mice (Fig. 5B and C). Essentially similar response curves were found with sera obtained 14 days after immunization (data not shown). PrP-specific antibody responses in $Prnp^{+/+}$ mice were slightly lower than those in $Prnp^{+/o}$ mice, which might be explained by a higher level of PrP-specific tolerance in $Prnp^{+/+}$ mice than in $Prnp^{+/o}$ mice.

Next we studied whether serum antibodies showing PrP-specific binding in an ELISA also bind the native form of PrP^{C} as expressed on the cell surface. To this end, peripheral blood was taken from tg33 mice overexpressing PrP on T lymphocytes (23), and CD3-positive T cells were tested for binding of serum IgM or IgG derived from immunized mice by FACS analysis.

Seven days after immunization of $Prnp^{o/o}$ mice, serum showed PrP^{C}-specific IgM binding that was slightly decreased by day 14, whereas strong PrP^{C}-specific IgG binding was detected on day 7 and was further increased by day 14, even beyond the binding strength of the positive control 6H4 (Fig. 6A and B). Reminiscent of the ELISA results described above, 7 days after immunization of $Prnp^{+/o}$ mice, serum showed PrP^{C}-specific IgM binding that was slightly lower than that of $Prnp^{o/o}$ mice and slightly higher than that of $Prnp^{+/+}$ mice (Fig. 6A), whereas 14 days after immunization, PrP^{C}-specific IgM was not detectable in sera of either $Prnp^{+/o}$ or $Prnp^{+/+}$ mice (Fig. 6B). Compared to that in sera of $Prnp^{o/o}$ mice, PrP^{C}-specific IgG binding was substantially reduced in the sera of $Prnp^{+/o}$ and $Prnp^{+/+}$ mice, whereas sera of $Prnp^{+/o}$ mice showed slightly higher binding than those of $Prnp^{+/+}$ mice. Interestingly, some PrP^{C}-specific IgG was still detectable 14 days after immunization (Fig. 6B).

To verify the specificity and reliability of the FACS method

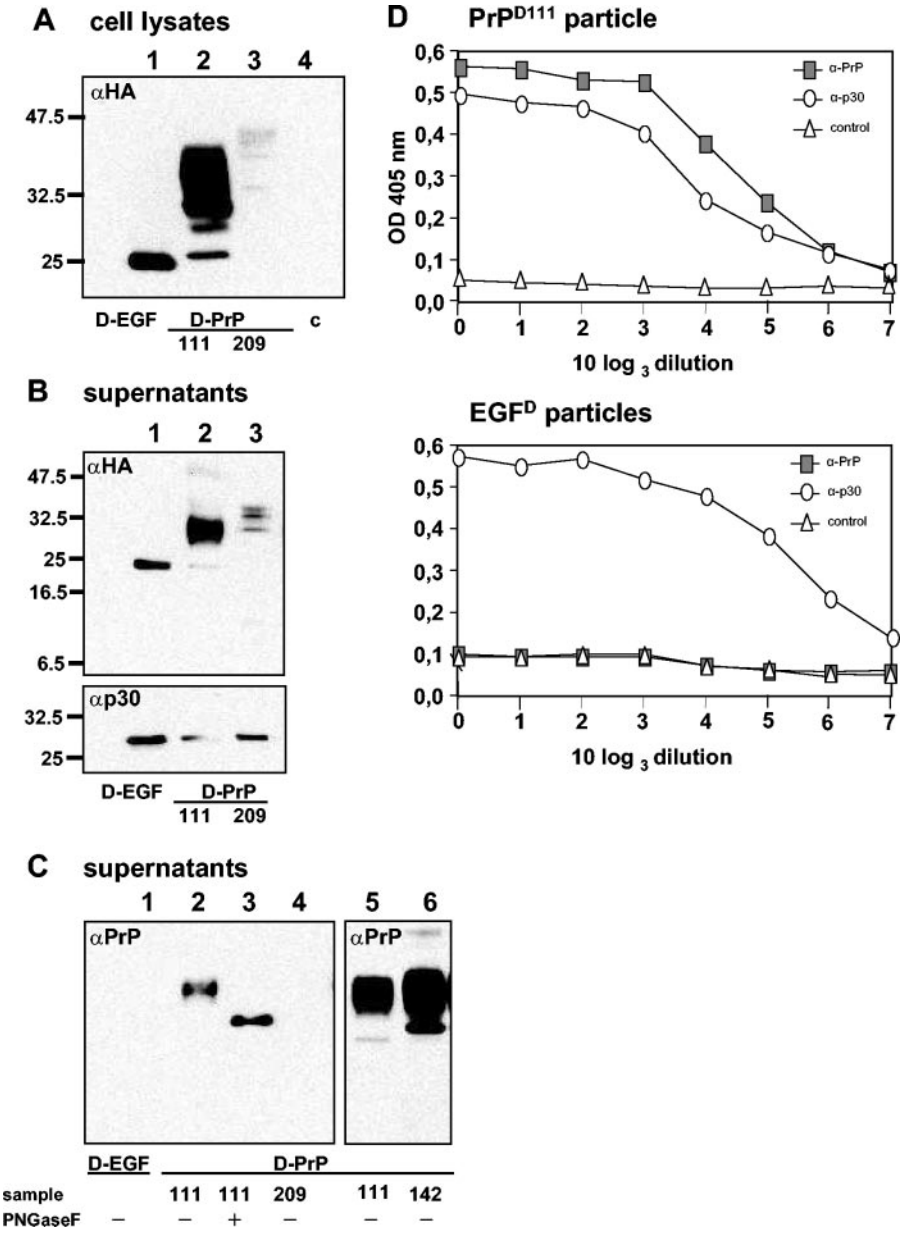

FIG. 3. The display proteins are incorporated into retroviral particles. Display and capsid proteins were detected by Western blot analysis with 16% polyacrylamide gels or by ELISA. (A) HEK-293FT cells were transfected with the pHIT60 plasmid and pD-EGF (lane 1), pD-PrP111 (lane 2), pD-PrP209 (lane 3), or an unrelated control plasmid (lane 4). Cell extracts were analyzed with the anti-HA (αHA) antibody. (B) Supernatants of HEK-293FT cells transfected with pHIT60/pD-EGF (lane 1), pHIT60/pD-PrP111 (lane 2), or pHIT60/pD-PrP209 (lane 3) were concentrated by low-speed centrifugation. Pellets were resuspended in PBS. Western blotting was performed with the anti-HA antibody in the upper blot and with anti-p30 serum to detect the MLV capsid in the lower blot. Volumes loaded corresponded to the following amounts of cell culture supernatant: 0.7 ml (lane 1, upper blot), 0.35 ml (lane 2, upper blot), and 13.5 ml (lane 3, upper blot). Volumes loaded on the lower blot corresponded to 1 ml of cell culture supernatant each. (C) Supernatants of HEK-293FT cells transfected with pHIT60/pD-EGF (lane 1), pHIT60/pD-PrP111 (lanes 2, 3, and 5), pHIT60/pD-PrP209 (lane 4), or pHIT60/pD-PrP142 (lane 6) were detected with the anti-PrP antibody 6H4. For PNGase F digestion, particles were equilibrated in denaturing buffer and incubated in the presence (lane 3) or absence (lane 2) of PNGase F. Volumes loaded on the gels correspond to 0.7 ml (lane 1), 0.35 ml (lanes 2 and 3), 13.5 ml (lane 4), 0.8 ml (lane 5), and 1.2 ml (lane 6) of cell culture supernatants. (D) Analysis of PrP^{D111} retroparticles (upper panel) and of EGF^{D} retroparticles (lower panel) by ELISA. Concentrated stocks of both particle types were applied to ELISA plates at the indicated dilutions. Virally expressed antigens were detected by use of the anti-PrP monoclonal antibody 6H4, polyclonal anti-p30 antiserum, or mouse preimmune serum. Data represent results from one of two experiments with similar results.

used for determination of PrP^{C} reactive antibodies, a number of control experiments were performed. First, N2A neuroblastoma cells and tg33-derived T cells incubated with 6H4 antibody or various different PrP-reactive immune sera showed very similar stainings, indicating that the tg33-based FACS method revealed binding of PrP^{C} as expressed on normal cells (data not shown). Second, a potential interindividual heterogeneity with respect to spontaneous PrP-specific antibody ti-

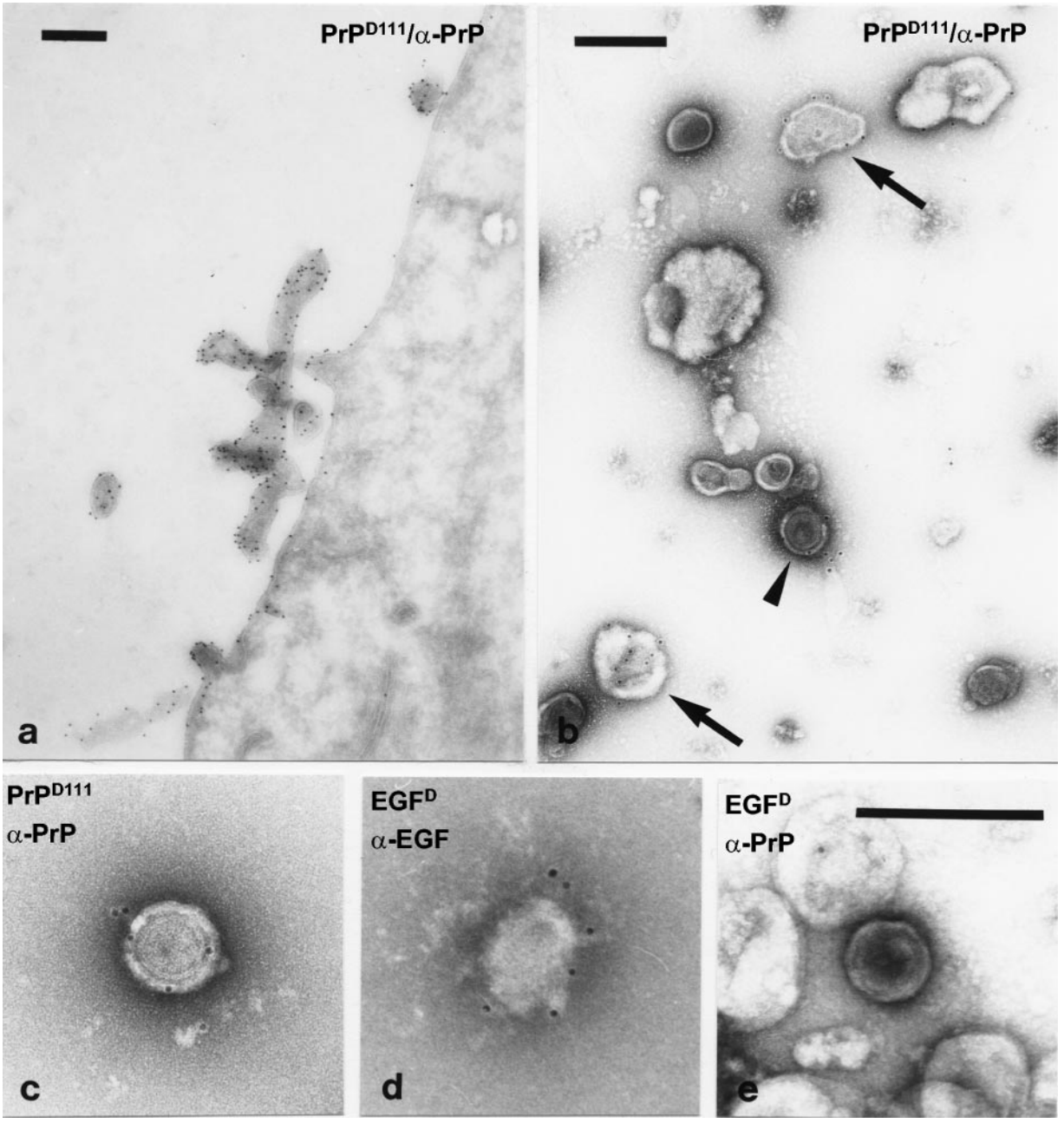

FIG. 4. Immunoelectron microscopic analysis of the particles. Sections through HEK-293FT producer cells transfected with pHIT60/pD-PrP111 (a) and PrP^{D111} retroparticles harvested from the cell culture supernatant and concentrated by low-speed centrifugation (b and c) were stained with the PrP-specific 6H4 antibody and a 10-nm-diameter gold particle-labeled anti-mouse IgG. EGF retroparticles (d and e) were harvested from pHIT60/pD-EGF-transfected 293FT cells and stained with the anti-EGF (d) or the 6H4 (e) antibody. Bars, 250 nm. Arrowheads indicate particles with the typical morphology of C-type retroviruses, and arrows indicate pleomorphic vesicles.

ters was assessed. To this end, individual preimmune sera and pools of preimmune sera derived from *Prnp*$^{+/+}$ and *Prnp*$^{o/o}$ mice were assayed for binding to tg33 cells in the tg33-based FACS assay. In no case was significant PrP binding of preimmune serum observed (Fig. 6C, right panel, and data not shown). Furthermore, the very narrow scattering of the blots of stainings with individual preimmune sera demonstrated the reliability and reproducibility of the FACS method used (Fig. 6C, bottom right panel). Third, for further verification of the PrP specificity of serum binding, we included *Prnp*$^{o/o}$-derived T cells in the FACS analysis as negative controls. Even when strong binding of tg33-derived T cells was observed, no IgG binding of *Prnp*$^{o/o}$-derived T cells was detected, with sera from either *Prnp*$^{o/o}$ or *Prnp*$^{+/+}$ mice (Fig. 6C, left panels). Finally, sera from *Prnp*$^{o/o}$ and *Prnp*$^{+/+}$ mice immunized with bacterially produced PrP^{REC} were analyzed by the tg33-based FACS assay (9, 22). In contrast to the sera obtained from immunizations with PrP^{D111} retroparticles, we could not detect any an-

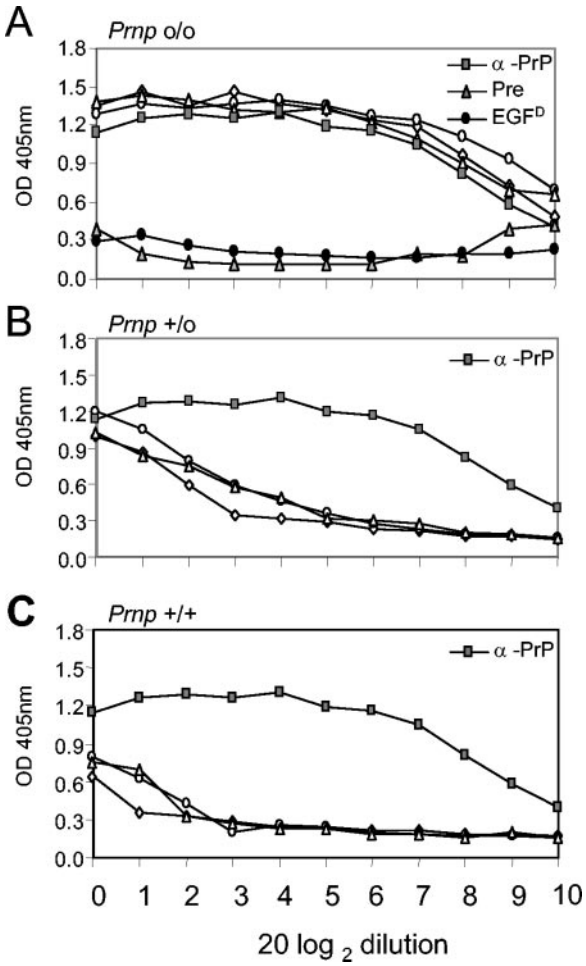

FIG. 5. Sera of mice immunized with PrP retroparticles specifically bind recombinant PrP in ELISA analysis. PrP^{D111} retroparticles devoid of adjuvant were injected i.v. into three individual mice of the $Prnp^{o/o}$ (A), $Prnp^{+/o}$ (B), or $Prnp^{+/+}$ (C) genotype (open symbols). Seven days after immunization, serum samples were taken and tested in $\log_2$ serial dilutions (20-fold predilution) for the presence of PrP-specific total Ig reactive against bacterially expressed $PrP^{REC121-231}$. As controls, the anti-PrP monoclonal antibody 6H4, preimmune serum, or sera from mice injected with EGF^D retroparticles were used. Results from one of two similar experiments are shown.

tibodies in $Prnp^{+/+}$ mice recognizing the native cell surface-exposed PrP (Fig. 6D). This failure of PrP^{REC} to circumvent tolerance in wild-type animals is in line with recently published data (22). In conclusion, PrP^{D111} retroparticles are good B-cell antigens as indicated by strong antibody responses induced in $Prnp^{o/o}$ mice. Furthermore, PrP^{D111} retroparticles can induce low but significant levels of native PrP^C-specific IgG antibodies in mice carrying one or two *Prnp* wild-type alleles, thus being superior to recombinant, bacterially expressed PrP.

Immunization of wild-type mice with PrP^{D111} retroparticles and different adjuvants. Next we assessed whether even higher antibody titers against native PrP^C could be induced if mice were immunized with retroparticles emulsified in various different adjuvants. To this end, mice were injected s.c. with PrP^{D111} retroparticles emulsified in CFA and boosted with antigen in IFA 2 weeks later. Seven days after primary immunization, wild-type ($Prnp^{+/+}$) mice showed PrP^C-specific IgM titers that generally were lower than those of i.v. immunized mice (Fig. 7). However, in single individuals this vaccination regimen resulted in increased native PrP^C-specific IgM titers (Fig. 7A, days 7 and 14) that switched to the IgG serotype upon boosting (Fig. 7A, days 28, 63, and 144). Furthermore, PrP^{D111} retroparticles emulsified in TiterMax, aluminum hydroxide (alum), or CpG1668 were also tested. Upon s.c. immunization of mice with PrP^{D111} retroparticles emulsified in TiterMax or alum, only low PrP^C-specific IgM titers were detectable at day 7, and they rapidly declined at later time points (data not shown). Under similar experimental conditions, CpG1668 did not show major adjuvant effects (data not shown). In summary, PrP^{D111} retroparticles are effective antigens, irrespective of whether they are emulsified in adjuvant or not. Notably, the coexistence of PrP^C-specific antibodies and of endogenous PrP^C in PrP^{D111} retroparticle-immunized mice did not result in obvious signs of autoimmune side effects.

DISCUSSION

Here we show that retroviral PrP-expressing particles represent a highly immunogenic PrP vaccine, which, for the first time, is capable of inducing anti-native PrP^C antibody titers in wild-type mice. Retroviral particles were selected as display vehicles based on their known ability to accommodate foreign transmembrane proteins in their envelope membrane. An important prerequisite for incorporation is efficient cell surface expression, thus increasing the likelihood of foreign transmembrane proteins being present at sites of viral budding. We used a previously successfully utilized system consisting of a signal peptide derived from the κ light chain and the PDGFR-derived transmembrane domain (4, 6). This approach resulted in efficient cell surface expression of the EGF molecule as well as of the C-terminal PrP domains (PrP111 and PrP142) and consequently in highly efficient particle incorporation. However, in this setting the complete PrP molecule (PrP209) showed strongly impaired cell surface transport and drastically reduced efficiency of incorporation into the particles. Besides the fact that the rather flexible disordered N-terminal domain of PrP may impede proper folding of the D-PrP209 molecule, while the globularly structured PrP111 and EGF molecules are well suited for expression in the retroviral membrane (24), reduced internalization rates and increased half-lives of PrP truncation mutants might facilitate the incorporation into VLPs (19).

A hallmark of propagation of the infectious agent of transmissible spongiform encephalopathies is the conversion of the cellular form of PrP into the pathogenic form PrP^{Sc}. PrP^{Sc} is thought to contain an increased amount of β-structure resulting from refolding of α-helices in PrP^C. Since a truncated PrP consisting of amino acids 90 to 231 seems to be sufficient to support prion propagation and thus to induce conversion of PrP^C to PrP^{Sc}, the D-PrP142 particle might be amenable to conversion into PrP^{Sc} (8). This possibility will be the subject of further studies to eventually develop PrP^{Sc}-displaying retroparticles.

Here we used the PrP retroparticles to evoke an immune response against PrP^C upon injection into $Prnp^{o/o}$ and wild-type mice. The use of virus-like particles is a well-established approach to generate subunit vaccines (18). Different types of viruses have been used, including hepatitis B virus and human

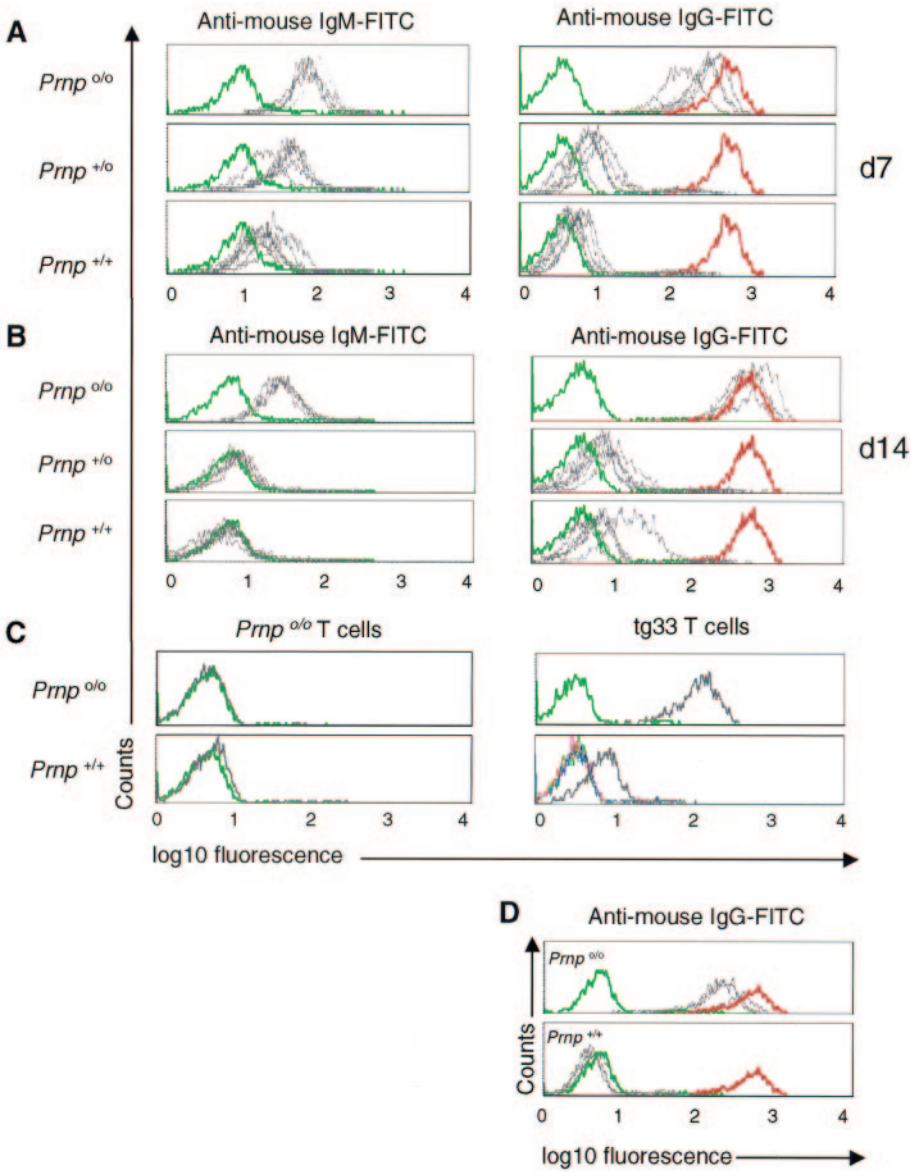

FIG. 6. Sera of mice immunized with PrP retroparticles specifically bind the native form of PrP as expressed on the cell surface of tg33-derived T cells. (A and B) Serum samples were taken 7 (A) or 14 (B) days after i.v. injection of PrP^{D111} retroparticles into $Prnp^{o/o}$, $Prnp^{+/o}$, or wild-type ($Prnp^{+/+}$) mice and analyzed for their reactivity against PrP as expressed on T cells derived from PrP-overexpressing tg33 transgenic mice. Five individuals per group were analyzed (gray lines). IgM (left panels) and IgG (right panels) subtypes were determined. Cells incubated with preimmune serum (green) or 6H4 (red) were used as controls. (C) Sera from immunized $Prnp^{o/o}$ or wild-type ($Prnp^{+/+}$) mice were tested for the reactivity of IgG subtypes with T cells from $Prnp^{o/o}$ mice (left panels, gray lines) or with T cells from tg33 mice (right panels, gray lines). Preimmune sera are shown in green in the left panels. Preimmune sera from five individual $Prnp^{+/+}$ mice (lower right panel, colored lines) or pooled preimmune sera from seven $Prnp^{o/o}$ mice (upper right panel, green line) were tested for IgG reactivity against PrP as expressed on tg33 T cells. (D) $Prnp^{o/o}$ mice immunized with PrP^{REC} in CFA and IFA mounted significant levels of anti-PrP antibodies, whereas $Prnp^{+/+}$ mice were unresponsive to immunizations. Bacterially expressed PrP^{REC} emulsified in CFA and IFA was injected into mice of the $Prnp^{o/o}$ and $Prnp^{+/+}$ genotypes (22). At 28 days after immunization, serum samples were analyzed for their IgG reactivity against PrP as expressed on tg33-derived T cells. Three individuals were analyzed per group (gray lines). Cells incubated with preimmune serum (green) or 6H4 (red) were used as controls. Histograms in all panels show PrP-specific binding gated on CD3-positive T cells.

papillomavirus. Retrovirus-like particles have been derived from HIV to develop novel candidate vaccines against AIDS (34). In that case the extracellular domain of the HIV Env protein gp120 was linked to the Epstein-Barr virus gp220/350 transmembrane domain to be incorporated into HIV-derived virus-like particles (5). Although the principle of this approach is similar to ours, we report here for the first time that retrovirus-like particles can be used to display antigens of cellular origin and to induce autoreactive antibody responses.

We assessed the antibody response in mice immunized with the PrP retroparticles by ELISA with bacterially expressed $PrP^{REC121-231}$ applied to plastic and by FACS analysis with T cells overexpressing PrP on the cell surface. A single i.v. immunization with PrP retroparticles was sufficient to induce

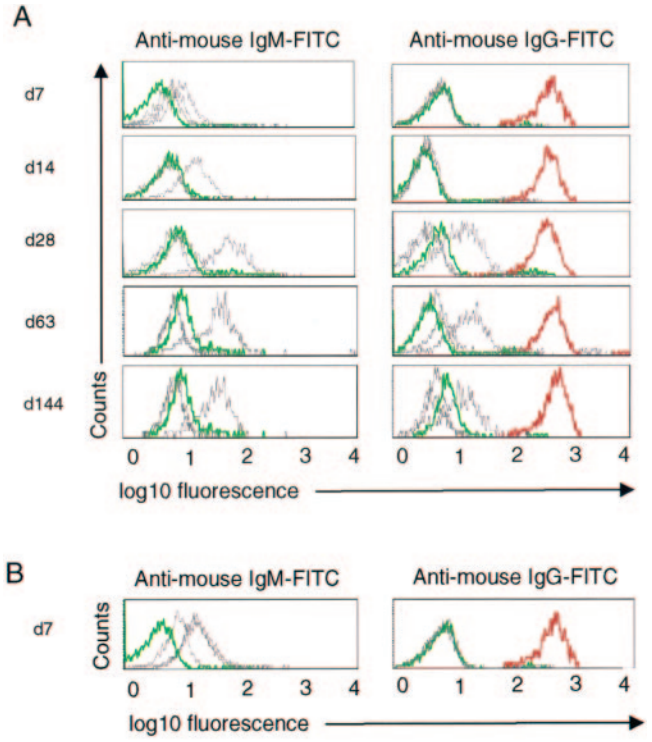

FIG. 7. *Prnp*$^{+/+}$ mice immunized with PrP retroparticles in CFA and IFA mount PrP-specific antibodies similar to those found after i.v. injection. *Prnp*$^{+/+}$ mice (three individuals) were injected s.c. with PrP^{D111} retroparticles emulsified in CFA and IFA (A) or injected i.v. with PrP^{D111} retroparticles devoid of adjuvant (B). PrP-specific binding of IgM (left panels) or IgG (right panels) was determined at the indicated days after immunization by FACS analysis with blood of tg33 transgenic mice overexpressing PrP specifically on T cells.

native PrP^{C} binding serum IgM and IgG antibodies in *Prnp*$^{o/o}$ mice, the latter of which showed at least as strong binding as the monoclonal anti-PrP IgG antibody 6H4. The induction of native PrP^{C}-specific IgM and IgG upon i.v. immunization with PrP retroparticles of wild-type mice is remarkable and has not been accomplished in a number of previous, rather disappointing, immunization studies (2, 9, 11, 12, 16, 25, 27, 28, 30). In a recent study, immunization with bacterially expressed recombinant full-length PrP emulsified in CFA resulted in the induction of antibodies directed against native PrP^{C} only if mice aberrantly expressing transgenic PrP under the control of an oligodendrocyte- and Schwann cell-specific promoter were used, whereas wild-type controls and all other PrP transgenic mice tested showed at best serum binding to recombinant PrP applied to plastic (22).

The magnitude of PrP-specific IgM responses upon i.v. PrP retroparticle immunization was inversely correlated with the number of *Prnp* alleles expressed; i.e., the highest level of PrP-specific IgM was induced in *Prnp*$^{o/o}$ mice, whereas intermediate and lower levels were detected in *Prnp*$^{o/+}$ and *Prnp*$^{+/+}$ mice, respectively. Nevertheless, it is remarkable that overall similar IgM levels were induced in mice of all three genotypes, especially at early time points. Obviously, immunologic host tolerance seems to be predominantly manifested on the T-cell level, so that in our experimental setting the magnitude of PrP^{C}-specific IgM responses is only gradually influenced by the expression level of the PrP self-determinant (1, 13, 31). Accordingly, the switch from the IgM to the IgG isotype of PrP^{C}-specific antibodies is less pronounced in wild-type animals than in *Prnp*$^{o/o}$ mice. Probably T-helper determinants accounting for the IgG switch in wild-type animals are provided by MLV-related antigens. In conclusion, it is remarkable that host tolerance left enough room for the induction of potentially autoreactive PrP-specific antibodies. This finding is in line with previous observations that PrP-specific B cells can develop in the presence of endogenously expressed PrP in 6H4μ transgenic mice (14). Further studies will reveal whether the induced antibody levels suffice to prevent prion disease and whether PrP retroparticles will hold promise as an antiprion vaccine.

ACKNOWLEDGMENTS

We thank K. Wüthrich for providing the bacterial expression construct pRSETa mPrP(121–231).

This work was supported by grants from the DFG (BU1301/1-1 and BU1301/1-2) to C.J.B. and by EU grant PRIOVAX (QLK2 CT2002 81399) to U.K., F.L.H., and A.A. F.L.H. is supported by the Bonizzi-Theler, Stammbach, and Leopoldina Foundations.

REFERENCES

1. **Adelstein, S., H. Pritchard-Briscoe, T. A. Anderson, J. Crosbie, G. Gammon, R. H. Loblay, A. Basten, and C. C. Goodnow.** 1991. Induction of self-tolerance in T cells but not B cells of transgenic mice expressing little self antigen. Science **251:**1223–1225.
2. **Arbel, M., V. Lavie, and B. Solomon.** 2003. Generation of antibodies against prion protein in wild-type mice via helix 1 peptide immunization. J. Neuroimmunol. **144:**38–45.
3. **Bueler, H., A. Aguzzi, A. Sailer, R. A. Greiner, P. Autenried, M. Aguet, and C. Weissmann.** 1993. Mice devoid of PrP are resistant to scrapie. Cell **73:** 1339–1347.
4. **Chesnut, J. D., A. R. Baytan, M. Russell, M. P. Chang, A. Bernard, I. H. Maxwell, and J. P. Hoeffler.** 1996. Selective isolation of transiently transfected cells from a mammalian cell population with vectors expressing a membrane anchored single-chain antibody. J. Immunol. Methods **193:**17–27.
5. **Deml, L., G. Kratochwil, N. Osterrieder, R. Knuchel, H. Wolf, and R. Wagner.** 1997. Increased incorporation of chimeric human immunodeficiency virus type 1 gp120 proteins into Pr55gag virus-like particles by an Epstein-Barr virus gp220/350-derived transmembrane domain. Virology **235:** 10–25.
6. **Douglas, J. T., C. R. Miller, M. Kim, I. Dmitriev, G. Mikheeva, V. Krasnykh, and D. T. Curiel.** 1999. A system for the propagation of adenoviral vectors with genetically modified receptor specificities. Nat. Biotechnol. **17:**470–475.
7. **Enari, M., E. Flechsig, and C. Weissmann.** 2001. Scrapie prion protein accumulation by scrapie-infected neuroblastoma cells abrogated by exposure to a prion protein antibody. Proc. Natl. Acad. Sci. USA **98:**9295–9299.
8. **Fischer, M., T. Rulicke, A. Raeber, A. Sailer, M. Moser, B. Oesch, S. Brandner, A. Aguzzi, and C. Weissmann.** 1996. Prion protein (PrP) with amino-proximal deletions restoring susceptibility of PrP knockout mice to scrapie. EMBO J. **15:**1255–1264.
9. **Gilch, S., F. Wopfner, I. Renner-Muller, E. Kremmer, C. Bauer, E. Wolf, G. Brem, M. H. Groschup, and H. M. Schatzl.** 2003. Polyclonal anti-PrP autoantibodies induced with dimeric PrP interfere efficiently with PrPSc propagation in prion-infected cells. J. Biol. Chem. **278:**18524–18531.
10. **Griffiths, G., K. Simons, G. Warren, and K. T. Tokuyasu.** 1983. Immunoelectron microscopy using thin, frozen sections: application to studies of the intracellular transport of Semliki Forest virus spike glycoproteins. Methods Enzymol. **96:**466–485.
11. **Hanan, E., O. Goren, M. Eshkenazy, and B. Solomon.** 2001. Immunomodulation of the human prion peptide 106–126 aggregation. Biochem. Biophys. Res. Commun. **280:**115–120.
12. **Hanan, E., S. A. Priola, and B. Solomon.** 2001. Antiaggregating antibody raised against human PrP 106–126 recognizes pathological and normal isoforms of the whole prion protein. Cell Mol. Neurobiol. **21:**693–703.
13. **Hartley, S. B., J. Crosbie, R. Brink, A. B. Kantor, A. Basten, and C. C. Goodnow.** 1991. Elimination from peripheral lymphoid tissues of self-reactive B lymphocytes recognizing membrane-bound antigens. Nature **353:**765–769.
14. **Heppner, F. L., C. Musahl, I. Arrighi, M. A. Klein, T. Rulicke, B. Oesch, R. M. Zinkernagel, U. Kalinke, and A. Aguzzi.** 2001. Prevention of scrapie pathogenesis by transgenic expression of anti-prion protein antibodies. Science **294:**178–182.

15. **Hornemann, S., C. Korth, B. Oesch, R. Riek, G. Wider, K. Wuthrich, and R. Glockshuber.** 1997. Recombinant full-length murine prion protein, mPrP(23–231): purification and spectroscopic characterization. FEBS Lett. **413:**277–281.
16. **Koller, M. F., T. Grau, and P. Christen.** 2002. Induction of antibodies against murine full-length prion protein in wild-type mice. J. Neuroimmunol. **132:** 113–116.
17. **Merten, C. A., M. Engelstaedter, C. J. Buchholz, and K. Cichutek.** 2003. Displaying epidermal growth factor on spleen necrosis virus-derived targeting vectors. Virology **305:**106–114.
18. **Noad, R., and P. Roy.** 2003. Virus-like particles as immunogens. Trends Microbiol. **11:**438–444.
19. **Nunziante, M., S. Gilch, and H. M. Schatzl.** 2003. Essential role of the prion protein N terminus in subcellular trafficking and half-life of cellular prion protein. J. Biol. Chem. **278:**3726–3734.
20. **Ott, D. E.** 1997. Cellular proteins in HIV virions. Rev. Med. Virol. **7:**167–180.
21. **Peretz, D., R. A. Williamson, K. Kaneko, J. Vergara, E. Leclerc, G. Schmitt-Ulms, I. R. Mehlhorn, G. Legname, M. R. Wormald, P. M. Rudd, R. A. Dwek, D. R. Burton, and S. B. Prusiner.** 2001. Antibodies inhibit prion propagation and clear cell cultures of prion infectivity. Nature **412:**739–743.
22. **Polymenidou, M., L. Heppner, E. C. Pellicioli, E. Urlich, G. Miele, N. Braun, F. Wophner, H. M. Schätzl, B. Becher, and A. Aguzzi.** 2004. Humoral immune response to native eukaryotic prion protein correlates with anti-prion protection. Proc. Natl. Acad. Sci. USA **101**:14670–14676.
23. **Raeber, A. J., A. Sailer, I. Hegyi, M. A. Klein, T. Rulicke, M. Fischer, S. Brandner, A. Aguzzi, and C. Weissmann.** 1999. Ectopic expression of prion protein (PrP) in T lymphocytes or hepatocytes of PrP knockout mice is insufficient to sustain prion replication. Proc. Natl. Acad. Sci. USA **96:** 3987–3992.
24. **Riek, R., S. Hornemann, G. Wider, M. Billeter, R. Glockshuber, and K. Wuthrich.** 1996. NMR structure of the mouse prion protein domain PrP(121–321). Nature **382:**180–182.
25. **Rosset, M. B., C. Ballerini, S. Gregoire, P. Metharom, C. Carnaud, and P. Aucouturier.** 2004. Breaking immune tolerance to the prion protein using prion protein peptides plus oligodeoxynucleotide-CpG in mice. J. Immunol. **172:**5168–5174.
26. **Sakalian, M., and E. Hunter.** 1998. Molecular events in the assembly of retrovirus particles. Adv. Exp. Med. Biol. **440:**329–339.
27. **Schwarz, A., O. Kratke, M. Burwinkel, C. Riemer, J. Schultz, P. Henklein, T. Bamme, and M. Baier.** 2003. Immunisation with a synthetic prion protein-derived peptide prolongs survival times of mice orally exposed to the scrapie agent. Neurosci. Lett. **350:**187–189.
28. **Sigurdsson, E. M., M. S. Sy, R. Li, H. Scholtzova, R. J. Kascsak, R. Kascsak, R. Carp, H. C. Meeker, B. Frangione, and T. Wisniewski.** 2003. Anti-prion antibodies for prophylaxis following prion exposure in mice. Neurosci. Lett. **336:**185–187.
29. **Soneoka, Y., P. M. Cannon, E. E. Ramsdale, J. C. Griffiths, G. Romano, S. M. Kingsman, and A. J. Kingsman.** 1995. A transient three-plasmid expression system for the production of high titer retroviral vectors. Nucleic Acids Res. **23:**628–633.
30. **Souan, L., Y. Tal, Y. Felling, I. R. Cohen, A. Taraboulos, and F. Mor.** 2001. Modulation of proteinase-K resistant prion protein by prion peptide immunization. Eur. J. Immunol. **31:**2338–2346.
31. **Tiegs, S. L., D. M. Russell, and D. Nemazee.** 1993. Receptor editing in self-reactive bone marrow B cells. J. Exp. Med. **177:**1009–1020.
32. **Tokuyasu, K. T., and S. J. Singer.** 1976. Improved procedures for immunoferritin labeling of ultrathin frozen sections. J. Cell Biol. **71:**894–906.
33. **White, A. R., P. Enever, M. Tayebi, R. Mushens, J. Linehan, S. Brandner, D. Anstee, J. Collinge, and S. Hawke.** 2003. Monoclonal antibodies inhibit prion replication and delay the development of prion disease. Nature **422:**80–83.
34. **Yao, Q., Z. Bu, A. Vzorov, C. Yang, and R. W. Compans.** 2003. Virus-like particle and DNA-based candidate AIDS vaccines. Vaccine **21:**638–643.
35. **Zahn, R., C. von Schroetter, and K. Wuthrich.** 1997. Human prion proteins expressed in Escherichia coli and purified by high-affinity column refolding. FEBS Lett. **417:**400–404.